

Energy Gap Closure of Crystalline Molecular Hydrogen with Pressure

Vitaly Gorelov,¹ Markus Holzmann,^{2,3} David M. Ceperley⁴, and Carlo Pierleoni^{1,5,*}

¹*Université Paris-Saclay, UVSQ, CNRS, CEA, Maison de la Simulation, 91191, Gif-sur-Yvette, France.*

²*Univ. Grenoble Alpes, CNRS, LPMMC, 38000 Grenoble, France*

³*Institut Laue-Langevin, BP 156, F-38042 Grenoble Cedex 9, France*

⁴*Department of Physics, University of Illinois at Urbana-Champaign, Urbana, Illinois 61801, USA*

⁵*Department of Physical and Chemical Sciences, University of L'Aquila, Via Vetoio 10, I-67010 L'Aquila, Italy*



(Received 15 November 2019; accepted 13 February 2020; published 16 March 2020)

We study the gap closure with pressure of crystalline molecular hydrogen. The gaps are obtained from grand-canonical quantum Monte Carlo methods properly extended to quantum and thermal crystals, simulated by coupled electron ion Monte Carlo methods. Nuclear zero point effects cause a large reduction in the gap (~ 2 eV). Depending on the structure, the fundamental indirect gap closes between 380 and 530 GPa for ideal crystals and 330–380 GPa for quantum crystals. Beyond this pressure the system enters into a bad metal phase where the density of states at the Fermi level increases with pressure up to ~ 450 –500 GPa when the direct gap closes. Our work partially supports the interpretation of recent experiments in high pressure hydrogen.

DOI: [10.1103/PhysRevLett.124.116401](https://doi.org/10.1103/PhysRevLett.124.116401)

The metallization of crystalline hydrogen under pressure has attracted considerable attention over the last century. Predicted to be stable in an atomic bcc lattice around 25 GPa, the mechanism for molecular dissociation was first discussed by Wigner and Huntington [1]. The search for its metallization has driven high pressure research until the recent [2], still debated [3–6], observation of reflective samples at 495 GPa in a diamond anvil cell (DAC) apparatus. Even though it is the simplest element and H_2 the simplest homonuclear molecule in nature, the study of hydrogen under extreme conditions has uncovered rich and unexpected physics [7–9].

The mechanism by which the insulating crystal transforms into a conducting crystal is still unclear. Experiments have difficulty in determining the crystalline structure and its evolution with pressure because of the low cross section to x rays [10–12] and the small volume of the samples for neutron scattering. Structural information is obtained indirectly through vibrational spectroscopy while the electronic structure is probed by optical measurements [13]. Direct measurements of static conductivity in the DAC remain inconclusive [14–19]. A complex phase diagram comprising up to at least four different molecular phases (from I to IV) with different vibrational spectra has been traced experimentally [8]. Recent experiments [2,19–22] searched for metallization at low temperature (≤ 100 K) while raising pressure in phase III. Considerable attention has also been paid to the higher temperature phase IV since its discovery [14,23–27]. The emerging picture is that the transparent insulating molecular phase III transforms into a strongly absorbing (in the visible) molecular phase at ~ 350 –360 GPa with different IR frequencies, first named

phase V [18] and later H_2 -PRE or phase VI [13,22], with semiconducting characteristics [28]. Hydrogen finally reaches a metallic phase with the observation of reflective samples at ~ 495 GPa [2], although disagreement concerning the pressure scale still remains [4,13,29]. New synchrotron infrared spectroscopy measurements [21] report a reversible collapse of the IR transmission spectrum at 427 GPa, interpreted as a first order transition to the metallic state.

In this Letter we investigate the closure of the electronic gap of candidate structures for phase III ($Cmca$ -12 and $C2/c$ -24) and phase IV ($Pc48$) [30,31] within a quantum Monte Carlo (QMC) framework [32]. For ideal structures, the fundamental gap decreases with pressure from ~ 3 –3.5 eV at ~ 250 GPa to a vanishing value ~ 380 GPa in the $Cmca$ -12 structure and ~ 530 GPa in the $C2/c$ -24 structure. Using coupled electron-ion Monte Carlo (CEIMC) calculations, we then include zero point motion (ZPM) and finite temperature effects of the nuclei within a first principles, nonperturbative path integral approach. Extending the grand canonical method [32] to quantum crystal at finite temperature, we observe a strong gap reduction of ~ 2 eV due to nuclear quantum effects (NQE) while temperature effects below 300 K are minor. At 200 K the fundamental indirect gap closes ~ 330 GPa for $Cmca$ -12 and ~ 380 GPa for $C2/c$ -24. Raising the temperature of $C2/c$ -24 to 290 K reduces the closure pressure to 340 GPa while decreasing it to 100 K does not give any noticeable effect. For both structures the direct gap, as obtained by unfolding of the supercell bands [33], remains open up to ~ 470 –500 GPa. Values for the $C2/c$ -24 structure are in agreement with recent experimental data [21], although we

cannot discuss the experimentally observed sudden closure at 427 GPa. Our new method for calculating energy gaps allows us to benchmark DFT functionals, not only for thermodynamics and structural properties, but also for excitation energies, important for predicting optical properties.

Method.—The primary information for theoretical investigations of solids are the crystalline structures. Candidate structures for high pressure phases have been obtained by *ab initio* random structural search methods [30,31,42,43]. For phase III we consider *C2/c-24* and *Cmca-12*, which are among the lowest free energy structures in ground state QMC calculations assuming harmonic phonon corrections (with DFT-PBE) [44–46]. For phase IV we consider only *Pc48*, since the recently proposed *Pca21* structure [43] is found to be rather similar to *Pc48* after geometry relaxation. We first consider ideal crystal structures (protons fixed at lattice sites) relaxed at constant pressure with the DFT-vdW-DF [47] functional. Quantum crystals, with protons represented by path integrals at finite temperature, are addressed with CEIMC at constant volume [48]. All systems considered have 96 protons in nearly cubic supercells. Optimized Slater-Jastrow-Backflow trial wave functions have been used for the CEIMC calculations [49]; details of the CEIMC simulations are reported in Ref. [50]. Averages over ionic positions for gaps are obtained using 40 statistically independent configurations from the CEIMC trajectories.

For a given fixed nuclear configuration, the fundamental energy gap is obtained by considering systems with a variable number of electrons $n \in [-6, 6]$, where $n = N_e - N_p$. For each system we perform reptation quantum Monte Carlo (RQMC) calculations with imaginary-time projection $t = 2.00$ and time step $\tau = 0.01 \text{ Ha}^{-1}$ for up to $6 \times 6 \times 6$ Monkhorst-Pack grid of twists. We check that those values are adequate for converging the band gaps within our resolution. The fundamental gap is obtained from grand-canonical twist-averaged boundary conditions (GCTABC) RQMC and corrected for finite size effects in leading and next-to-leading order [32].

Extending calculations of the fundamental gaps to quantum crystals, the trace over nuclear degrees of freedom must be taken with care. In the semiclassical approximation [33], the fundamental gap is the smallest electronic excitation energy that occurs from quantum or thermal fluctuations of the lattice. Strictly speaking this gap is always closed, since the probability of a proton configuration with a metallic character is never exactly zero. For dense molecular hydrogen phonon energies are $\sim 0.1\text{--}0.5 \text{ eV}$ [31]. ZPM dominates for $T \leq 1000 \text{ K}$, so the semiclassical approach is not appropriate. Electronic energies should be averaged over the nuclear configurations according to their thermal distribution. The gap will be given by the minimum of the average excitation energies, always larger than the semiclassical gap. Figure 4 illustrates typical results for the

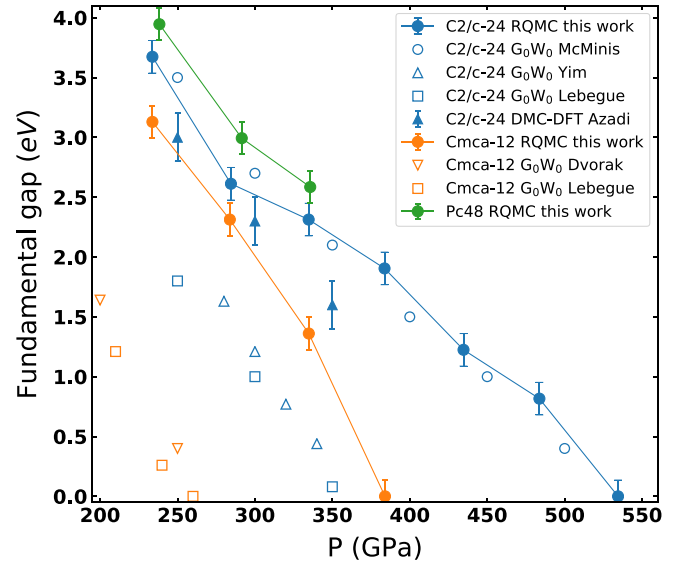


FIG. 1. Fundamental energy gap for ideal crystals. This work (closed circles): *C2/c-24* (blue), *Cmca-12* (orange), and *Pc48* (green), GW results for *C2/c-24* (open blue circles [44]). These structures were optimized with the vdW-DF functional. QMC for *C2/c-24* optimized with the BLYP from Ref. [51] (closed blue triangles). GW results from Refs. [53–55] for *C2/c-24* (blue) and *Cmca-12* (orange) optimized with the PBE functional. Note that pressures from RQMC are 10–15 GPa lower than the nominal optimization pressure.

integrated density of states as a function of (electronic) chemical potential. The gap of the quantum crystal can be directly read off from the width of the incompressible region. More details are given in Ref. [33].

Results.—Figure 1 shows estimates of the fundamental gap for ideal crystals versus pressure. The gap decreases with pressure in a similar fashion for all structures: *Cmca-12* has the smallest gap, followed by *C2/c-24* and by *Pc48*. We find reasonable agreement with the QMC estimates of Refs. [51,52]. References [53–55] report smaller values of the gap based on GW. We believe this disagreement is primarily due to the lattice geometry that has been optimized at constant pressure with PBE in Refs. [53–55] and with vdW-DF in the present work. It has been previously observed that PBE optimized geometries have longer H_2 bonds and smaller gap values at the DFT level [56,57]. This propagates into G_0W_0 . Indeed, GW results from structures optimized with vdW-DF [44] are in excellent agreement with our predictions.

Values of the fundamental gap from GCTABC for quantum crystals at various temperatures and pressures are shown in Fig. 2: they are smaller by $\sim 2 \text{ eV}$ with respect to the ideal crystal. ZPM is almost entirely responsible for this reduction. Note that the gap hardly changes from 300 to 200 K within our estimated errors. Similar to ideal crystals, the *Cmca-12* gap is smaller than the *C2/c-24* gap at $T = 200 \text{ K}$, the former closing $\sim 340 \text{ GPa}$, while the latter at higher pressures $\sim 380 \text{ GPa}$. As for the *Pc48* structure at

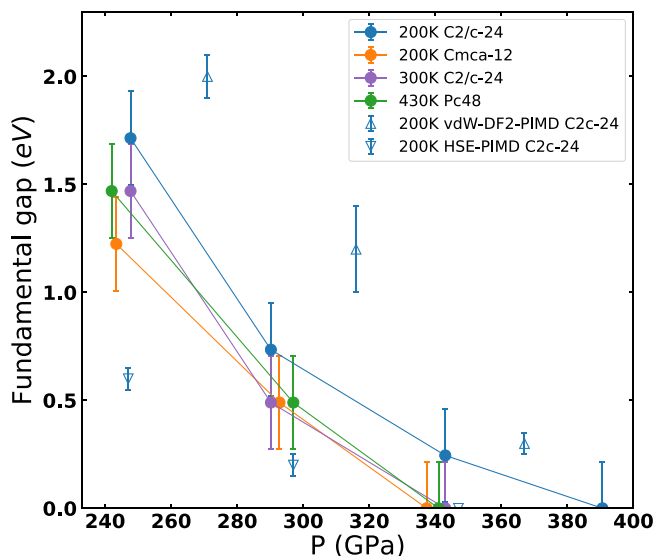


FIG. 2. The fundamental gap of quantum crystals at finite temperature. Closed circles indicate results from this work, for the three structures at various temperature as detailed in the legend. PIMD-DFT results at $T = 200$ K are obtained with two different XC approximations, namely, the HSE (downward open triangles) and the vdW-DF2 (upward open triangles) and the semiclassical averaging are reported for comparison [56].

$T = 430$ K (phase IV) the gap is slightly below values for $C2/c-24$ at 200 K. Our results show that the electronic gap is fairly independent of the specific crystalline structure of the molecular quantum crystals. We also report gap values for $C2/c-24$ at $T = 200$ K from path integral molecular dynamics (PIMD) [56] with two different DFT functionals, namely, the HSE [58] and vdW-DF2 [59]. As vdW-DF2 underestimates the molecular bond lengths of the ideal crystalline structure [57], its PIMD configurations are expected to bias the electronic gap towards larger values. Our results do not agree with predictions of Ref. [60] (not shown) yielding a metallic state for $C2/c-24$ at 300 GPa and 300 K, and predict substantially larger gap reduction for $C2/c-24$ quantum crystals than Ref. [61]. However, those works are based on less controlled assumptions such as using “scissor corrected” BLYP [62,63] band structure and an *ad hoc* procedure for including nuclear motion.

For all structures considered the observed fundamental gap is indirect. An estimate of the direct gap can be obtained by unfolding the band structure of the supercell [33]. Figure 3 shows the direct gap for both $C2/c-24$ and $Cmca-12$ structures. While for the indirect gap $Cmca-12$ is always lower than $C2/c-24$, the direct gap is systematically larger. The difference between the direct and indirect gap is of ~ 1 eV for $C2/c-24$, and of ~ 2 eV for $Cmca-12$. Closure of the direct gaps, obtained by linear extrapolation, occurs ~ 450 GPa in $C2/c-24$ and ~ 500 GPa in $Cmca-12$. Hence for both structures we observe an intermediate pressure region where the fundamental indirect gap is closed but the direct vertical gap remains open

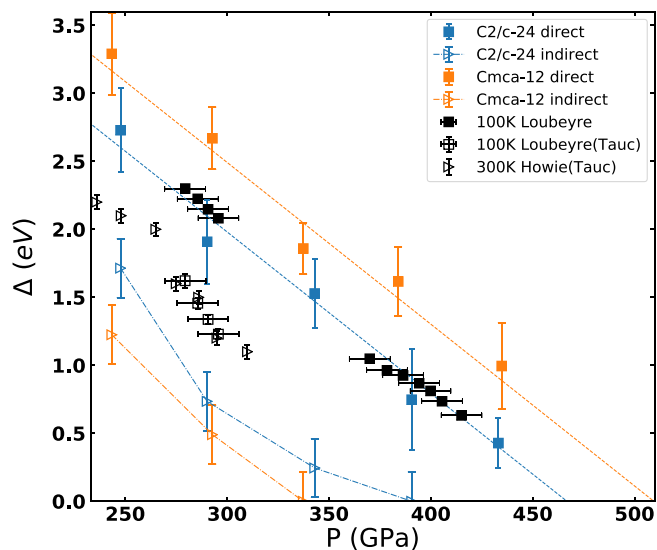


FIG. 3. Direct (closed symbols) and indirect (open symbols) gaps of quantum crystals. GCTABC-RQMC at $T = 200$ K: $C2/c-24$ indirect (blue triangles), direct (blue squares); $Cmca-12$ indirect (orange triangles), direct (orange squares). Experiments: indirect gap from the Tauc analysis at $T = 100$ K (phase III), (black squares) [64] and at 300 (phase IV), (black triangles) [17,24]; direct gap at 100 K (black squares) [21,64].

and decreases linearly with pressure. In this region, we expect the density of states around the Fermi level to increase progressively with pressure, as qualitatively reported in Ref. [50]. This indicates the formation of a bad metal with properties similar to a semimetal upon closure of the indirect gap, a scenario strongly supporting the recently proposed experimental picture [28] (see also Refs. [13,22]). The nonvanishing direct gap naturally explains the reported observation of absorbing (black) hydrogen around 320–360 GPa (depending on the experimental pressure scale) [64].

Figure 3 also shows the experimental estimates of both indirect and direct gaps from optical absorption. Measuring indirect gaps is difficult in hydrogen since samples are very thin and the optical signal from phonon-assisted absorption is too low to be detected [16,19]. The indirect gap value has been extracted from a Tauc analysis of the absorption profiles at 300 K (phase IV) [17,24] and 100 K (phase III) [25,64] assuming the low energy absorption spectrum can be reliably extrapolated to zero energy. [65]. Conversely, the direct gap at 100 K (phase III) has been associated with the absorption edge at lower pressure [64] or with full absorption at higher pressure [21] and corresponds roughly to the energy where the absorption coefficient equals $30\,000\text{ cm}^{-1}$. The direct gap of $C2/c-24$ structure is in agreement with the experimental data up to 425 GPa, where experiments report a collapse of the gap value ascribed to the metallization transition [21]. Our results do not allow us to predict this transition, but rule out $C2/c-24$ and $Cmca-12$ for this new metallic phase [66]. For the indirect

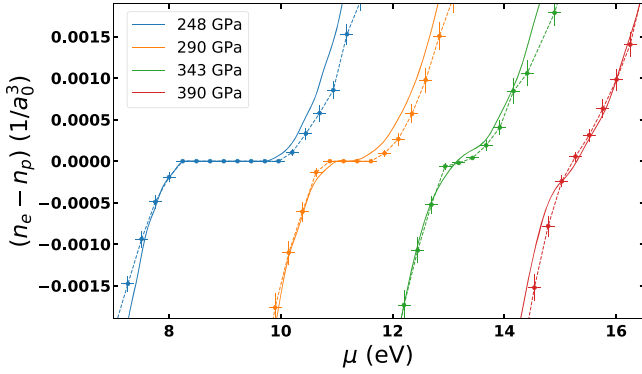


FIG. 4. Integrated density of states for $C2/c-24$ quantum crystals at 200 K from GCTABC-RQMC (points) and the HSE (smooth lines) at various pressures.

gap we predict $\sim 0.3\text{--}0.5$ eV smaller values than in experiments. However, the Tauc analysis of Refs. [17,24,64] does not consider the energy of the emitted or absorbed phonons, which should be comparable to the observed discrepancy. However, excitonic effects and exciton-phonon coupling, neglected within the present approach, need to be addressed for this level of precision. In agreement with our findings, the experimental indirect gap depends little on both temperature and structure [67].

Next, we explore optical properties computed using the Kubo-Greenwood (KG) framework with Kohn-Sham (KS) orbitals. To reduce the bias of the underlying DFT functional, we have benchmarked several XC approximations to reproduce the behavior of the QMC density of states close to the gap. In Fig. 4 for $C2/c-24$ at 200 K, we compare the electronic excess density $n_e - n_p$ as a function of electronic chemical potential μ from QMC and from DFT-HSE [68]. The observed plateau at $n_e - n_p = 0$ is the signature of the indirect gap. Deviations from the plateau on both sides characterize the density of states of the valence and conduction band close to the band edges. As shown in Fig. 4 the HSE approximation provides slightly smaller values of the fundamental gap and reproduces reasonably well the integrated density of states from GCTABC around the Fermi energy (more details are in Ref. [33]). We therefore employed the HSE to compute optical properties exploiting the KGEC code [69] in the QuantumEspresso suite [70]. For thermal and quantum crystals considered here, the William-Lax (WL) semiclassical (SC) approximation [71–75] is not appropriate as already discussed. Instead of a joint density of states based on excitation energies for each nuclear configuration entering the WL expression, we have used the corresponding one based on electronic energies averaged over ionic ZPM, more appropriate for low temperatures [33]. In Fig. 5 we compare the absorption profiles for $C2/c-24$ at $T = 200$ K and different pressures [76] to experimental profiles from Refs. [21,64] at $T = 100$ K. We observe a higher absorption than in experiments at comparable pressure, which cannot be

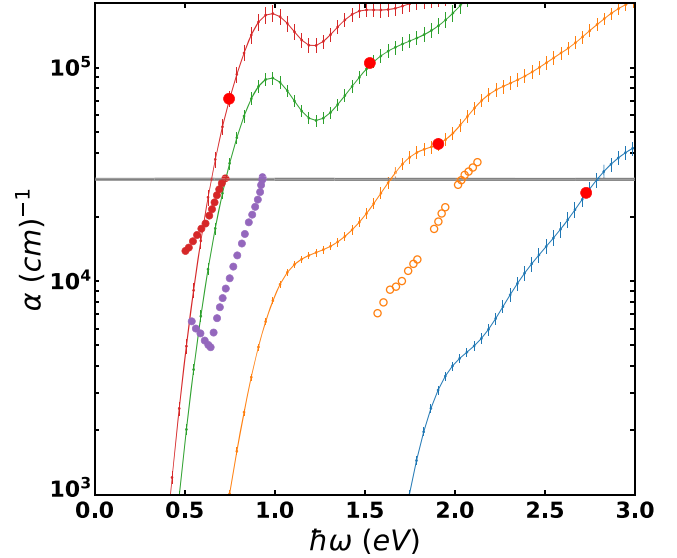


FIG. 5. Absorption spectra from the HSE band structure for $C2/c-24$ quantum crystals (solid lines) and comparison with the available experimental profiles (opened and filled circles). The spectra from the HSE has been shifted in energy by an amount equal to the difference between QMC and the HSE direct gap. The reported pressure are as in Fig. 4 (see the colors). The red dots indicate the location in energy of the direct gap of Fig. 3. Experimental pressures are 296 GPa, open orange circles [64] (corrected by 20 GPa [21]); 386 GPa, magenta filled circles and 406 GPa, red filled circles [21].

explained by the temperature difference. We marked each predicted profile with a red dot at the energy corresponding to the observed direct gap and we report a thick horizontal line at $30\,000\text{ cm}^{-1}$ the value of the absorption used in the experiments to extract the value of the direct gap. Our results at lower pressures are in reasonable agreement with this criterion. However at the higher pressure, absorption at the energy gap is about 2–3 times higher than $30\,000\text{ cm}^{-1}$.

Conclusions.—We have studied the closure of the fundamental gap with pressure of candidate structures of molecular hydrogen in phase III ($C2/c-24$ and $Cmca-12$) and phase IV ($Pc48$) entirely based on quantum Monte Carlo simulations. For ideal structures our gap values are in excellent agreement with GW prediction [44]. Considering quantum nuclei at finite temperature, we observe a strong reduction of the energy gap with respect to the ideal structures at the same pressure (~ 2 eV) caused by ZPM. At 200 K the fundamental (indirect) gap closes at $\sim 370\text{--}380$ GPa for $C2/c-24$ and at ~ 340 GPa for $Cmca-12$. We observe a reasonable agreement with experimental determinations of indirect gaps from optical absorption. The direct gap remains open until ~ 450 GPa for $C2/c-24$ and ~ 500 GPa for $Cmca-12$. In this range of pressure the system is a bad metal (or semimetal) suggesting a scenario that qualitatively supports recent experiments [19,20,22,28]. In Refs. [19,28] no discontinuities in the Raman vibrational spectrum are reported when entering

the semimetallic phase, while in Refs. [20,22] new IR vibron peaks are reported in this pressure range and ascribed to a structural phase transition. They have been tentatively assigned to a transition from the $C2/c-24$ to the $Cmca-12$ structure [22]. Our present results, supplemented by free energy calculations [77], do not disprove this hypothesis. Our predictions for direct gap are in good agreement with the experimental data at $T = 100$ K [21,64]. However our absorption profiles do not agree as well with the experimental behavior. This disagreement remains an open question.

We thank Paul Loubeyre, Mikhail Eremets, Mario Santoro, and Michele Nardone for useful suggestions. D. M. C. was supported by DOE Grant No. NA DE-NA0001789 and by the Fondation NanoSciences (Grenoble). V. G. and C. P. were supported by the Agence Nationale de la Recherche (ANR) France, under the program “Accueil de Chercheurs de Haut Niveau 2015” project: HyLightExtreme. Computer time was provided by the PRACE Project No. 2016143296, ISCRAB (IsB17_MMCRHY) computer allocation at CINECA Italy, the high-performance computer resources from Grand Equipement National de Calcul Intensif (GENCI) Allocation 2018-A0030910282, by an allocation of the Blue Waters sustained petascale computing project, supported by the National Science Foundation (Grant No. OCI 07- 25070) and the State of Illinois, and by the Froggy platform of CIMENT, Grenoble (Rhône-Alpes CPER07-13 CIRA and ANR-10-EQPX-29-01).

*carlo.pierleoni@aquila.infn.it

- [1] E. Wigner and H. B. Huntington, *J. Chem. Phys.* **3**, 764 (1935).
- [2] R. P. Dias and I. F. Silvera, *Science* **355**, 715 (2017).
- [3] A. F. Goncharov and V. V. Struzhkin, *Science* **357**, eaam9736 (2017).
- [4] P. Loubeyre, F. Occelli, and P. Dumas, arXiv:1702.07192.
- [5] X.-D. Liu, P. Dalladay-Simpson, R. T. Howie, B. Li, and E. Gregoryanz, *Science* **357**, eaan2286 (2017).
- [6] I. Silvera and R. Dias, *Science* **357**, eaan1215 (2017).
- [7] H. K. Mao and R. Hemley, *Rev. Mod. Phys.* **66**, 671 (1994).
- [8] J. M. McMahon, M. A. Morales, C. Pierleoni, and D. M. Ceperley, *Rev. Mod. Phys.* **84**, 1607 (2012).
- [9] W. J. Nellis, *Rep. Prog. Phys.* **69**, 1479 (2006).
- [10] P. Loubeyre, R. LeToullec, D. Hausermann, M. Hanfland, R. J. Hemley, H. K. Mao, and L. W. Finger, *Nature (London)* **383**, 702 (1996).
- [11] C. Ji, B. Li, W. Liu, J. S. Smith, A. Majumdar, W. Luo, R. Ahuja, J. Shu, J. Wang, S. Sinogeikin, Y. Meng, V. B. Prakapenka, E. Greenberg, R. Xu, X. Huang, W. Yang, G. Shen, W. L. Mao, and H.-K. Mao, *Nature (London)* **573**, 558 (2019).
- [12] L. Dubrovinsky, N. Dubrovinskaia, and M. I. Katsnelson, arXiv:1910.10772.
- [13] I. Silvera and R. P. Dias, *J. Phys. Condens. Matter* **30**, 254003 (2018).
- [14] M. I. Eremets and I. A. Troyan, *Nat. Mater.* **10**, 927 (2011).
- [15] W. J. Nellis, A. L. Ruoff, and I. F. Silvera, arXiv:1201.0407.
- [16] A. F. Goncharov and V. V. Struzhkin, <https://arxiv.org/pdf/1207.6643.pdf>.
- [17] A. F. Goncharov, J. S. Tse, H. Wang, J. Yang, V. V. Struzhkin, R. T. Howie, and E. Gregoryanz, *Phys. Rev. B* **87**, 024101 (2013).
- [18] M. I. Eremets, I. A. Troyan, and A. P. Drozdov, arXiv:1601.04479.
- [19] M. Eremets, A. P. Drozdov, P. Kong, and H. Wang, arXiv:1708.05217.
- [20] R. P. Dias, O. Noked, and I. F. Silvera, arXiv:1603.02162.
- [21] P. Loubeyre, F. Occelli, and P. Dumas, *Nature (London)* **577**, 631 (2020).
- [22] R. P. Dias, O. Noked, and I. F. Silvera, *Phys. Rev. B* **100**, 184112 (2019).
- [23] R. T. Howie, T. Scheler, C. L. Guillaume, and E. Gregoryanz, *Phys. Rev. B* **86**, 214104 (2012).
- [24] R. T. Howie, C. L. Guillaume, T. Scheler, A. F. Goncharov, and E. Gregoryanz, *Phys. Rev. Lett.* **108**, 125501 (2012).
- [25] C. S. Zha, Z. Liu, and R. J. Hemley, *Phys. Rev. Lett.* **108**, 146402 (2012).
- [26] P. Loubeyre, F. Occelli, and P. Dumas, *Phys. Rev. B* **87**, 134101 (2013).
- [27] R. T. Howie, P. Dalladay-Simpson, and E. Gregoryanz, *Nat. Mater.* **14**, 495 (2015).
- [28] M. I. Eremets, A. P. Drozdov, P. P. Kong, and H. Wang, *Nat. Phys.*, <https://doi.org/10.1038/s41567-019-0646-x> (2019).
- [29] M. I. Eremets and A. P. Drozdov, arXiv:1601.04479.
- [30] C. J. Pickard and R. J. Needs, *Nat. Phys.* **3**, 473 (2007).
- [31] C. J. Pickard, M. Martinez-Canales, and R. J. Needs, *Phys. Rev. B* **85**, 214114 (2012).
- [32] Y. Yang, V. Gorelov, C. Pierleoni, D. M. Ceperley, and M. Holzmann, *Phys. Rev. B* **101**, 085115 (2020).
- [33] See Supplemental Material at <http://link.aps.org/supplemental/10.1103/PhysRevLett.124.116401> for more information about: computing band gap for thermal crystals, Tauc analysis of experimental indirect gap, benchmark of some XC functionals and Kubo-Greenwood optical calculations for thermal crystals, which includes Refs. [35–41].
- [34] R. M. Martin, L. Reining, and D. M. Ceperley, *Interacting Electrons: Theory and Computational Approaches* (Cambridge University Press, Cambridge, England, 2016).
- [35] J. P. Perdew, *Int. J. Quantum Chem.* **28**, 497 (1985).
- [36] C. Lin, F. H. Zong, and D. M. Ceperley, *Phys. Rev. E* **64**, 016702 (2001).
- [37] M. Holzmann, B. Bernu, V. Olevano, R. M. Martin, and D. M. Ceperley, *Phys. Rev. B* **79**, 041308(R) (2009).
- [38] G. Grosso and G. Parravicini, *Solid State Physics*, 2nd ed. (Academic Press, Amsterdam, 2014).
- [39] F. Wooten, *Optical Properties of Solids* (Academic Press, New York, 1972).
- [40] M. A. Morales, R. Clay, C. Pierleoni, and D. M. Ceperley, *Entropy* **16**, 287 (2014).
- [41] J. Tauc, R. Grigorovici, and A. Vancu, *Physica Status Solidi (B)* **15**, 627 (1966).
- [42] C. Pickard, M. Martinez-Canales, and R. Needs, *Phys. Rev. B* **85**, 214114 (2012).
- [43] B. Monserrat, N. D. Drummond, P. Dalladay-Simpson, R. T. Howie, P. L. Rios, E. Gregoryanz, C. J. Pickard, and R. J. Needs, *Phys. Rev. Lett.* **120**, 255701 (2018).

- [44] J. McMinis, R. C. Clay, D. Lee, and M. A. Morales, *Phys. Rev. Lett.* **114**, 105305 (2015).
- [45] S. Azadi, B. Monserrat, W. M. C. Foulkes, and R. J. Needs, *Phys. Rev. Lett.* **112**, 165501 (2014).
- [46] J. P. Perdew, K. Burke, and M. Ernzerhof, *Phys. Rev. Lett.* **78**, 1396 (1997).
- [47] M. Dion, H. Rydberg, E. Schröder, D. C. Langreth, and B. I. Lundqvist, *Phys. Rev. Lett.* **95**, 109902 (2005).
- [48] We have checked that the stress tensor in the constant volume CEIMC run remains diagonal with the same diagonal elements within our statistical noise.
- [49] C. Pierleoni, M. A. Morales, G. Rillo, M. Holzmann, and D. M. Ceperley, *Proc. Natl. Acad. Sci. U.S.A.* **113**, 4953 (2016).
- [50] G. Rillo, M. A. Morales, D. M. Ceperley, and C. Pierleoni, *J. Chem. Phys.* **148**, 102314 (2018).
- [51] S. Azadi, N. D. Drummond, and W. M. C. Foulkes, *Phys. Rev. B* **95**, 035142 (2017).
- [52] The observed small difference, in particular at the higher pressure, is probably due to the different XC approximation used for geometry optimization, vdW-DF in our case, BLYP in Ref. [51] and different size extrapolation.
- [53] S. Lebègue, C. Araujo, D. Kim, M. Ramzan, H. Mao, and R. Ahuja, *Proc. Natl. Acad. Sci. U.S.A.* **109**, 9766 (2012).
- [54] Y. L. R. J. H. Wai-Leung Yim, H. Shi, and J. S. Tse, in *Correlations in Condensed Matter under Extreme Conditions*, edited by G. A. Editors and A. L. Magna (Springer International Publishing, AG, 2017), Chap. 9, pp. 107–126.
- [55] M. Dvorak, X.-J. Chen, and Z. Wu, *Phys. Rev. B* **90**, 035103 (2014).
- [56] M. A. Morales, J. M. McMahon, C. Pierleoni, and D. M. Ceperley, *Phys. Rev. B* **87**, 184107 (2013).
- [57] R. C. Clay, J. Mcminis, J. M. McMahon, C. Pierleoni, D. M. Ceperley, and M. A. Morales, *Phys. Rev. B* **89**, 184106 (2014).
- [58] J. Heyd, J. E. Peralta, G. E. Scuseria, and R. L. Martin, *J. Chem. Phys.* **123**, 174101 (2005).
- [59] K. Lee, É. Murray, L. Kong, B. Lundqvist, and D. Langreth, *Phys. Rev. B* **82**, 081101 (2010).
- [60] S. Azadi, R. Singh, and T. D. Kühne, *J. Comput. Chem.* **39**, 262 (2018).
- [61] X.-Z. Li, B. Walker, M. I. J. Probert, C. J. Pickard, R. J. Needs, and A. Michaelides, *J. Phys. Condens. Matter* **25**, 085402 (2013).
- [62] A. D. Becke, *Phys. Rev. A* **38**, 3098 (1988).
- [63] C. Lee, W. Yang, and R. G. Parr, *Phys. Rev. B* **37**, 785 (1998).
- [64] P. Loubeyre, F. Occelli, and R. LeToullec, *Nature (London)* **416**, 613 (2002).
- [65] We have re-analyzed the spectra of Ref. [64] to extract the value of the indirect gap from a Tauc plot [41], as was performed in Ref. [17] for the data from Ref. [24]. Details are given in Ref. [33].
- [66] Our estimates of the direct gap could be biased by ~ 0.3 eV due to the discreteness of our twist grid. Correcting for this bias will place the experimental data in between the $C2/c-24$ and $Cmca-12$ predictions.
- [67] Note that the pressure values of Ref. [64] have been recently corrected [21].
- [68] This quantity is closely related to the integrated density of states.
- [69] L. Calderín, V. V. Karasiev, and S. B. Trickey, *Comput. Phys. Commun.* **221**, 118 (2017).
- [70] P. Giannozzi *et al.*, *J. Phys. Condens. Matter* **29**, 465901 (2017).
- [71] F. Williams, *Phys. Rev.* **82**, 281 (1951).
- [72] M. Lax, *J. Chem. Phys.* **20**, 1752 (1952).
- [73] C. E. Patrick and F. Giustino, *J. Phys. Condens. Matter* **26**, 365503 (2014).
- [74] M. Zacharias, C. E. Patrick, and F. Giustino, *Phys. Rev. Lett.* **115**, 177401 (2015).
- [75] M. Zacharias and F. Giustino, *Phys. Rev. B* **94**, 075125 (2016).
- [76] To partially correct for the HSE inaccuracy, we shifted the energy scale by the difference between the QMC and HSE gap.
- [77] C. Pierleoni (to be published).